Negative refraction in semiconductor metamaterials based on quantum cascade laser design for the mid-IR and THz spectral range

J. Radovanović[1*], S. Ramović[1], A. Daničić[2] and V. Milanović[1]

[1]School of Electrical Engineering, University of Belgrade, Serbia
[2]Vinča Institute of Nuclear Sciences, University of Belgrade, Serbia
[*]corresponding author: radovanovic@etf.bg.ac.rs

Abstract

We have considered the realization of metamaterials based on semiconductor quantum nanostructures, in particular, with the structural arrangement as in quantum cascade laser (QCL) designed to achieve optical gain in the mid-infrared and terahertz part of the spectrum. The entire structure is placed in a strong external magnetic field which facilitates the attainment of sufficient population inversion, necessary to manipulate the permittivity and enable left-handed regime.

1. Introduction

In recent years a new type of artificial electromagnetic composites termed metamaterials (MTMs) has been extensively studied and developed. The broad range of configurations of these materials has introduced a variety of otherwise unexpected physical phenomena, among which the realization of negative refractive index and cloaking effect have been among the most interesting ones [1]. Composite metamaterial elements are patterned in a periodic array to form metamaterials, and the dimensions of unit cells, which metamaterials are composed of, are significantly less than the wavelength, on the order of tenths of wavelengths. Thus metamaterials can be considered as an effective medium and are well described by magnetic permeability and electric permittivity, in accordance with the macroscopic form of Maxwell's equations.

The advent of MTMs enabled control of electromagnetic properties of materials, going beyond the limit that is attainable with naturally existing structures. This is especially important for the technologically relevant terahertz frequency regime, because the tools that are necessary to construct devices operating within this spectral range are mainly lacking. Considerable efforts are underway to fill this 'THz gap' in view of the useful potential applications of the THz radiation. Techniques to control and manipulate THz waves are lagging behind, but moderate progress has been made in THz generation and detection and one of the recent examples is the THz quantum cascade laser.

In this paper we have considered the realization of metamaterials with the structural composition as in quantum cascade lasers which are intended to exhibit negative refraction in the mid-infrared and terahertz part of the spectrum. Our metamaterials belong to low-loss and active optical materials, and are made of very thin GaAs/AlGaAs layers, whose configuration corresponds to quantum cascade laser. They are subjected to very strong magnetic fields which enable modulation of the optical gain by discretizing the in-plane electron motion and thus make it possible to obtain negative index of refraction.

2. Theoretical consideration

Quantum cascade laser is a low-dimensional semiconductor quantum structure that consists of series of identical stages, allowing each electron to emit many photons during its transit through the structure. This scheme provides excellent laser performance in terms of optical gain and output power, thus it has been successfully utilized in many different applications (high-sensitivity gas sensing, infrared imaging, security monitoring and non-invasive medical diagnostics) in the mid-infrared and far-infrared part of the electromagnetic spectrum [2-7]. However, in spite of impressive properties demonstrated in the mid infrared, the operation in the THz part of the spectrum is subject to inherent limitations. Therefore, a lot of research effort has been invested recently into developing different approaches to overcome these limitations.

Many of the proposed and experimentally demonstrated metamaterials are based on inclusions of smart metallic films, wires, or spheres and therefore exhibit high optical losses which are detrimental to their performance and considerably limit their usefulness [8-10]. One of the major challenges in new metamaterial development is to design active metamaterials, i.e. to compensate the losses by adding gain. Active metamaterials, which comprise thin layers of semiconductors materials with particular layout,

may be used to realize substantial optical gain via carrier injection at frequencies of interest [8,9,11,12]. Specifically, the QCL-like structural profile allows for significant tunability of output properties and offers prospects for efficient engineering of effective permittivity [2,4,13,14]. The relative magnetic permeability of a semiconductor-based non-magnetic material is $\mu = 1$, while the dielectric permittivity tensor may be written as [9]:

$$\|\varepsilon\| = \begin{Vmatrix} \varepsilon_{\|} & 0 & 0 \\ 0 & \varepsilon_{\|} & 0 \\ 0 & 0 & \varepsilon_{\perp} \end{Vmatrix} \tag{1}$$

This form is valid for quantum well based semiconductor nanostructures which exhibit strong anisotropy of optical properties. Here, $\varepsilon_{\|}$ is the permittivity component along the quantum well planes, and is equal to the average permittivity of the background materials (ε_b), while $\varepsilon_{\perp}$ describes the interaction along the growth (*z*) axis and may be represented by the Lorentz model [15]:

$$\varepsilon_{\perp} = \varepsilon_b + \frac{e^2}{\varepsilon_0 \hbar L} \sum_{m<n} \left(N_{s,m} - N_{s,n} \right) \cdot \frac{\left| z_{m,n} \right|^2}{\left(\omega_{nm} - \omega \right) - i\gamma_{nm}} \tag{2}$$

Here, L is the length of the unit cell in *z* direction, $N_{s,i}$ represents the electron sheet density in *i*-th state, ω_{nm} is the resonant transition frequency between states *n* and *m*, ω is the frequency of the input light, γ_{nm} denotes the transition linewidth, while z_{mn} is the transition matrix element between states *n* and *m*. According to Eq. (2), the normal component of dielectric permittivity strongly depends on the populations of electron energy levels. Our goal was to meet the criteria for negative refraction, which in case of anisotropic, single-negative, metamaterial read [16]:

$$\varepsilon_{\|} > 0, \quad \mathrm{Re}\left(\varepsilon_{\perp} \right) < 0 \tag{3}$$

In the case of a passive configuration, when the upper levels are less occupied than the lower ones, both parts, the imaginary and the real one, of $\varepsilon_{\perp}$ are always positive. But in the active configuration, the total dielectric permittivity could be made negative by controlling the carrier distribution (Eq. (2)). Hence, in order to obtain negative values of the real part of $\varepsilon_{\perp}$, one clearly has to achieve high enough population inversion $N_{s,n} > N_{s,m}$ to cancel out the background term and reverse the sign of the real part of Eq. (2).

The active region of the QCL structures under consideration consists of two and three coupled quantum wells, for the terahertz and mid-infrared part of the electromagnetic spectrum, respectively, biased by an external electric field. Each period of the structure has three crucial energy states, and the laser transitions occur between the upper (*n*=3) and the lower (*n*=2) energy state. The main scattering mechanism is the electron-LO-phonon scattering, which is responsible for depopulation of the lower laser state. The active region is surrounded by the emitter/collector barriers, which enable injection of carriers from the preceding active region/extraction from the lower subband.

The direct use of LO-phonon scattering for lower state depopulation offers two advantages. First, when the ground energy state (*n*=1) is separated from the lower laser state (*n*=2) by the resonant LO-phonon energy, depopulation can is extremely fast. Second, the large energy separation between these two states provides intrinsic protection against thermal backfilling of the lower radiative state. Both properties are very important for lasers at longer wavelengths (which are within our subject of interest), because they allow for higher temperature operation. Therefore, our semiconductor QCL structures are designed so that the energy difference between the states E_2 and E_1 is approximately equal to LO-phonon energy in order to maintaining high population inversion.

In normal operating conditions, the electron motion in QCL structure is quantized along the growth direction only and free in the direction parallel to QW planes (*x*-*y*). When a strong perpendicular magnetic field is introduced, the in-plane electron motion becomes discretized as well, and continuous two-dimensional energy subbands are split into series of discrete Landau levels (LLs) whose energies, with band nonparabolicity included, are given by [17-21]:

$$E_{n,l}(B) = E_{n0} + (l + \frac{1}{2}) \frac{\hbar e B}{m_{\|,n}(E_{n0})} - \frac{1}{8} \left[\left(8l^2 + 8l + 5 \right) \left\langle \alpha_0 \right\rangle + \left(l^2 + l + 1 \right) \left\langle \beta_0 \right\rangle \right] \left(\hbar \omega_c \right)^2 \tag{4}$$

where $\omega_c = eB / m_{\|,n}(E_{n0})$ is the cyclotron frequency, E_{n0} the in-plane energy of the state *n* for zero in-plane wave vector ($k_{\|} = 0$), *l*=0,1,2,... is the Landau index, $m_{\|n}(E_{n0})$ represents the energy-dependent in-plane electron effective mass and *B* is the external magnetic field. The mean values of non-parabolicity parameters $\left\langle \alpha_0 \right\rangle$, $\left\langle \beta_0 \right\rangle$, averaged over the z-coordinate, are given according to [20]. It is obvious from Eq. (4) that the energy separations between Landau levels depends on the strength of the applied magnetic field which influences all the relevant relaxation processes in the structure and consequently the lifetime of carriers in the upper laser level. This enables one to control the population inversion in the active region and to influence the overall operation of the QCL structure, as described in detail in Ref.[18]. Here, such effect may be used to tune the carrier relaxation rates and their distributions over LLs which is important because it strongly affects the permittivity.

To calculate the normal component of the permittivity, one must first find the electron distribution over all Landau levels, by solving the nonlinear system of rate equations [11]:

$$\frac{\partial N_f}{\partial t} = \overline{f}_f \sum_{i \neq f} N_i W_{E_i \to E_f} - N_f \sum_{i \neq f} \overline{f}_i W_{E_f \to E_i} \qquad (5)$$

where indices i,f run over all Landau levels in all of the periods of the QCL and the probability that the state i is unoccupied is given by $\overline{f}_i = 1 - \pi\hbar/(eB) N_i$ according to the Fermi-Dirac distribution. The periodic QCL design enables solving the system of rate equations in a simplified form as described in [18]. Each state and its LLs can be associated with one of the periods of the QCL due to the wave-function localization properties. We assume that inside the cascade there is a globally linear potential variation, which enables the use of periodic boundary conditions for the particle surface densities. Each period is assumed to have an identical set of N Landau levels, with identical electron distributions. Out of the total of N, there are $N-1$ linearly independent equations, so one of them is replaced by the particle conservation law: $\sum_i N_i = N_S$, where N_S is the total electron sheet density

3. Results and Discussion

The calculations are performed for GaAs/AlGaAs quantum cascade laser structures, designed to emit radiation at mid-infrared and THz frequencies, under the influence of an intense external magnetic field.

The first structure under consideration is a GaAs/$Al_{0.38}Ga_{0.62}As$ QCL, comprising three quantum wells per period, gain-optimized by the genetic algorithm for emission at $\lambda = 7.3\mu m$ [12]. Starting from the left well the layer widths are: 11Å, 32Å, 39Å, 23Å, 38Å and the barrier height is U_B=0.317eV. The applied electric field in the z-direction is K=48kV/cm, and the minima of energy subbands (prior to the application of external magnetic field) are at $E_1(k_{\|}=0) = 0.083\text{eV}$, $E_2(k_{\|}=0) = 0.119\text{eV}$ and $E_3(k_{\|}=0) = 0.290\text{eV}$. The material parameters used in calculations are: $m^* = 0.0665\, m_0$ (m_0 is the free electron mass), $\gamma_{nm} = 5$ meV, $\varepsilon_b \approx 13$ and the one period length (the active region plus the corresponding injector/collector) L=500Å.

Oscillations of the relaxation rate with magnetic field for transitions from the ground LL of the third subband, into which the majority of carriers are injected, into the two sets of LLs of the two lower subbands are very pronounced. The prominent peaks are found at values of the magnetic field which satisfy the resonance conditions for LO phonon emission. On the contrary, when the arrangement of Landau levels is such that there is no level situated at $\approx \hbar\omega_{LO}$ below the state (3,0), this type of scattering is inhibited, and the lifetime of the upper laser state is increased. When the current injection is constant, the modulation of lifetimes of all the states in the system results in either a suppression or an enhancement of population inversion between states (3,0) and (2,0). Thus, for magnetic field values at which the configuration of relevant electronic states leads to maximally enhanced relaxation rate from the (3,0) state, there is a huge drop in the optical gain, and conversely, for certain values of B there appears a peak of the gain. The total permittivity is calculated according to Eq. (2), and two particular cases, one for magnetic fields which enhances the population inversion and one where a minima of population inversion is found, are presented in Fig. 1. The injection current is kept constant for all displayed magnetic field strengths. It is not necessary to reach extremely high values of the optical gain in order to obtain negative real part of the permittivity. As shown, this can be accomplished for regular carrier sheet densities, but at specific values of magnetic at which the population inversion is enhanced.

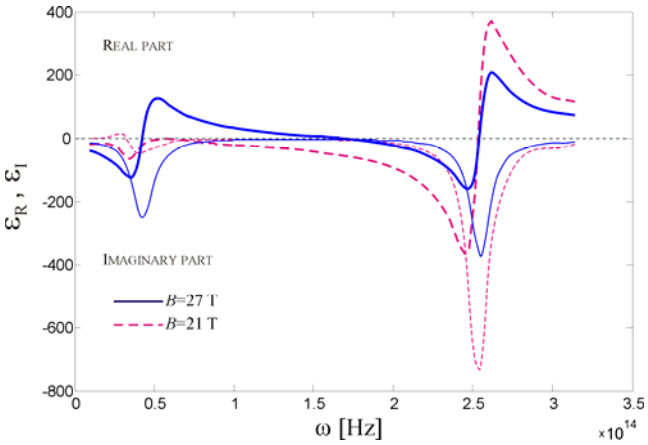

Figure 1: The dependence of $\varepsilon_\perp$ on frequency in a mid-IR QCL for various magnetic field values, at N_S=1·10^{11}cm^{-2} and T=300K

The realistic effects of band non-parabolicity influence the energy separation between the levels relevant for the radiative transition, thus the resonant wavelength becomes dependent on the magnetic field. This allows for the small shift of wavelength at which the minima of ε_R and ε_I are achieved and it may be used for fine-tuning of the permittivity.

Figure 2 illustrates how the frequency range $\Delta\omega$, at which metamaterial behaves as left-handed, depends on the electron sheet densities and on magnetic field values. Dark blue regions correspond to situations at which negative-refraction cannot be obtained. Even if the structure is exposed to very high values of B, in these cases it is impossible to reach high enough population inversion in QCL to obtain a left-handed regime. We observe that it is necessary to set (by doping) the total electron sheet density to at least $N_s \approx 1\cdot10^{10}$ cm^{-2}, so that the metamaterial could enter the desired working regime for some magnetic fields. The increase in the doping level leads to spreading of the magnetic field range at which negative-refraction may be reached, and the frequency range at which material behaves as left-handed. The widest range $\Delta\omega$ occurs at magnetic field which enhances the population inversion (B=27T) and

it is quite large for all electron sheet densities above $N_{s(\min)}$. On the other hand, the narrowest bandwidth corresponds to B at which the configuration of relevant electronic states leads to a maximally enhanced relaxation rate from the (3,0) state and that is for B=30T

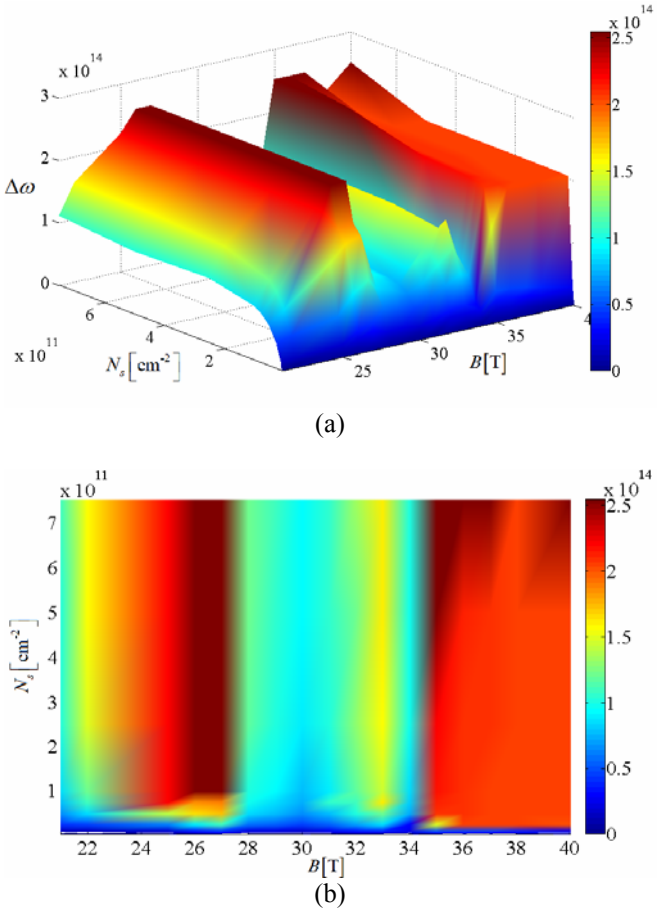

Figure 2: (a) The dependence of $\Delta\omega$ on electron sheet densities for various magnetic field values presented as a 3D plot, at T=300K. (b) Orthographic projection of the dependence of $\Delta\omega$ on electron sheet densities N_S and magnetic field B.

In order to present some results of our ongoing work, which is focused on designing negative-index metamaterials based on terahertz QCLs, we describe the second analyzed structure. It is a GaAs/$Al_{0.15}Ga_{0.85}As$ QCL, comprising two quantum wells per period, designed to emit radiation at 4.6 THz [13]. The layer widths are 56, 71, 31, 167 Å, starting from the emitter towards the collector barrier, and the electric field is 17 kVcm^{-1}. The calculated energy difference between subbands 3 and 2 is 20.9 meV, while the difference between the lower laser state and the ground state is $E_2 - E_1 = 36\text{meV} \approx \hbar\omega_{LO}$. The conduction band diagram of one period of the structure is illustrated in Figure 3.

In modeling this THz QCL an additional nonradiative relaxation mechanism that affects the operation of the structure must be included: the interface roughness scattering [22,23]. This type of scattering must be accounted for in calculations because of the small difference between adjacent levels. The numerical parameters used in calculations (in addition to the above parameters for MIR QCL) are: U_B=0.125eV, relevant parameters for interface roughness scattering Δ=1.5Å (height of roughness) and Λ=60Å (correlation length).

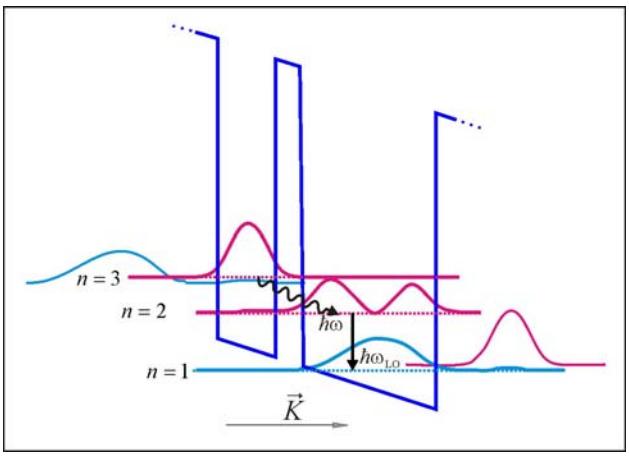

Figure 3: Conduction band profile of a single period of two-well THz quantum cascade laser.

The dependence of the modal gain on the applied magnetic field for this structure is illustrated in Figure 4. The oscillations of the relaxation rate with B are again very pronounced, with two distinct peaks around B=9 T and B=17.5 T. When the arrangement of LLs is such that there is no level situated near the state (3,0), or at $\approx \hbar\omega_{LO}$ below it, the relevant scattering rates are minimal and the modal gain is significantly increased.

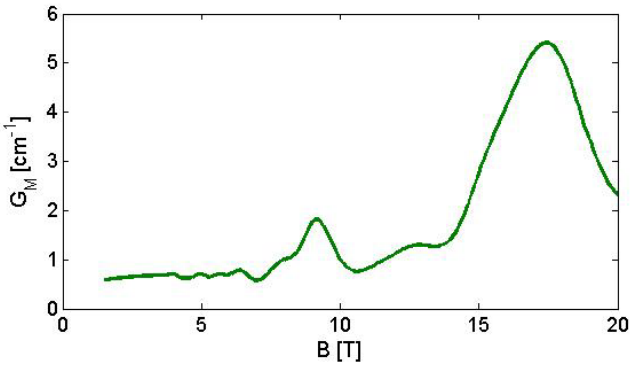

Figure 4: The modal gain in a THz QCL as a function of the applied magnetic field at N_S=2.2·10^{12}cm^{-2} and T=77K

For magnetic field which maximizes the optical gain in this structure (B=17.4T), with high enough doping level (N_S=5·10^{11}cm^{-2}) it is possible to achieve negative values of the real part of $\varepsilon_\perp$ (Fig. 5).

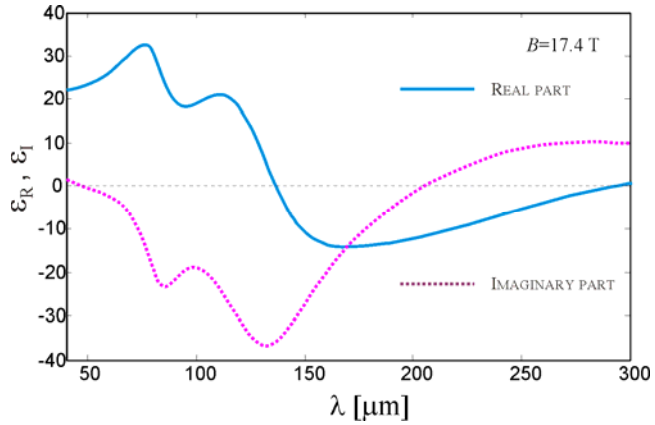

Figure 5: The dependence of $\varepsilon_{\perp}$ on the radiation wavelength in a THz QCL, for B=17.4 T at N_S=5·10^{11}cm^{-2} and T=77K.

4. Conclusions

The calculations are performed for GaAs/AlGaAs quantum cascade laser structures, design to emit radiation at mid-infrared and THz frequencies, under the influence of an intense external magnetic field. Their energies depend on the field, which, together with the fact that scattering rates between states are sensitive to their energy spacing, enables one to selectively enhance or inhibit different relaxation channels by varying the magnetic-field strength, which translates into a field-induced modulation of the population inversion.

The results presented in this paper show that it is possible to obtain a sufficiently high degree of population inversion to invert the sign of $\mathrm{Re}(\varepsilon_{\perp})$ i.e. to obtain its negative values. In fact, for mid-infrared structure we can even distinguish two frequency ranges where the structure behaves as left-handed. For certain magnetic fields that enhance the optical gain, those two regions may even merge into a very wide one. However, the fact that the structure is exposed to a very strong magnetic field, may not be sufficient condition to obtain high enough population inversion in the QCL active region to enable the left-handed regime. The other condition that must be fulfilled is the total electron sheet density, which in our case needs to be at least $N_s \approx 1 \cdot 10^{10}$ cm^{-2}. An increase in the doping level leads to extension of magnetic field range at which negative-refraction is achieved and the corresponding frequency span.

For the THz metamaterial structure we have also achieved the desired operating regime, but only for higher doping levels and applied magnetic fields which maximize the optical gain. This is due to a large background permittivity of GaAs, so our future work will focus on exploring other semiconductor materials, with lower background permittivity, in order to design left-handed metamaterials which require much lower magnetic field strengths.

Acknowledgements

This work was supported by the Ministry of Science (Republic of Serbia), ev. no. III 45010 and NATO SfP Grant, ref. no. ISEG.EAP.SFPP 984068.

References

[1] D. Schurig, J. J. Mock, B. J. Justice, S. A. Cummer, J. B. Pendry, A. F. Starr, D. R. Smith, Metamaterial electromagnetic cloak at microwave frequencies, *Science* 314: 977-980, 2006.

[2] J. Faist, F. Capasso, D. L. Sivco, C. Sirtori, A. L. Hutchinson , A. Y. Cho, Quantum Cascade Laser, *Science* 264: 553-556, 1994.

[3] C. Gmachl, F. Capasso, D. L. Sivco, A. Y. Cho, Recent progress in quantum cascade lasers and applications, *Rep. Prog. Phys.* 64, 1533-1601, 2001.

[4] B. S. Williams, Terahertz quantum-cascade lasers, *Nat. Photonics* 1: 517-525, 2007.

[5] O. Drachenko, S. Winnerl, H. Schneider, M. Helm, J. Wosnitza, J. Leotin, Compact magnetospectrometer for pulsed magnets based on infrared quantum cascade lasers, *Rev. Sci. Intrum.* 82**:** 033108 , 2011.

[6] A. Hugi, R. Maulini, J. Faist, Topical review—external cavity quantum cascade laser, *Semicond. Sci. Technol.* 25: 083001 , 2010.

[7] R.F. Curl, F. Capasso, C. Gmachl, A. A. Kosterev, B. McManus, R. Lewicki, M. Pusharsky, G. Wysocki, F. K. Tittel, Quantum cascade lasers in chemical physics, *Chem. Phys. Lett.* 487: 1-18, 2010.

[8] P. Ginzburg, M. Orenstein, Metal-free quantum-based metamaterial for surface plasmon polariton guiding with amplification, *J. Appl. Phys*. 104: 063513 (1-5), 2008.

[9] P. Ginzburg, M. Orenstein, Nonmetallic left-handed material based on negative-positive anisotropy in low-dimensional quantum structures, *J. Appl. Phys*. 103: 083105 (1-5), 2008.

[10] V. M. Shalaev , Optical negative-index metamaterials, *Nat. Photonics* 1: 41-48, 2007.

[11] I. Savić, N. Vukmirović, Z. Ikonić, D. Indjin, R. W. Kelsall, P. Harrison, V. Milanović, Density matrix theory of transport and gain in quantum cascade lasers in a magnetic field , *Phys. Rev. B* 76: 165310 , 2007.

[12] S. Ramović, J. Radovanović, V. Milanović, Tunable Semiconductor Metamaterials Based On Quantum Cascade Laser Layout Assisted By Strong Magnetic Field, *J. Appl. Phys*. 110: 123704 (1-5), 2011.

[13] S. Kumar, C. W. I. Chan, Q. Hu, J. Reno, Two-well terahertz quantum-cascade laser with direct intrawell-phonon depopulation, *Appl. Phys. Lett*. 95: 14110 (1-3), 2009.

[14] A. Wade, G. Fedorov, D. Smirnov, S. Kumar, B. S. Williams, Q. Hu, J. L. Reno, Magnetic-field-assisted terahertz quantum cascade laser operating up to 225 K, *Nature Photon*. 3: 41-45, 2007.

[15] P. Basu, *Theory of Optical Processes in Semiconductors: Bulk and Microstructures*, Clarendon Press, Oxford, 1997.

[16] V. A. Podolskiy, E. E. Narimanov, Strongly anisotropic waveguide as a nonmagnetic left-handed system, *Phys. Rev B* 71: 201101R (1-4), 2005.

[17] J. Radovanović, V. Milanović, Z. Ikonić, D. Indjin, P. Harrison, Electron-phonon relaxation rates and optical gain in a quantum cascade laser in a magnetic field, *J. Appl. Phys.* 97: 103109 (1-5), 2005.

[18] A. Daničić, J. Radovanović, V. Milanović, D. Indjin, Z. Ikonić, Optimization and magnetic-field tunability of quantum cascade laser for applications in trace gas detection and monitoring, *J. Phys. D: Appl. Phys*. 43: 045101 (1-8), 2010.

[19] J. Radovanović, A.Mirčetić, V. Milanović, Z. Ikonić, D. Indjin, P. Harrison, R.W. Kelsall, Influence of the active region design on output characteristics of GaAs/AlGaAs quantum cascade lasers in a strong magnetic field, *Semicon. Sci. Technol.* 21: 215-220, 2006.

[20] U. Ekenberg, Nonparabolicity effects in a quantum well: Sublevel shift, parallel mass, and Landau levels, *Phys. Rev. B* 40: 7714-7726, 1989

[21] J.Radovanović and Milanović, Quantum Cascade Laser: Applications In Chemical Detection And Environmental Monitoring, *Nucl. Technol. Radiat.* 24: 75-81, 2009.

[22] A. Leuliet, A. Vasanelli, A. Wade, G. Fedorov, D. Smirnov, G. Bastard and C. Sirtori, Electron scattering spectroscopy by a high magnetic field in quantum cascade lasers, *Phys. Rev. B* 73: 085311 (1-9), 2006.

[23] T. Unuma, M. Yoshita, T. Noda, H. Sakaki and H. Akiyama, Intersubband absorption linewidth in GaAs quantum wells due to scattering by interface roughness, phonons, alloy disorder, and impurities, *J. Appl. Phys* 93: 1586 (1-12), 2003.